Nanoscale Infrared Spectroscopy Reveals Nanoplastics at 5000 m Depth in the South Atlantic Ocean

Bert Weckhuysen (b.m.weckhuysen@uu.nl)
Utrecht University https://orcid.org/0000-0001-5245-1426
Iris ten Have
Utrecht University
Florian Meirer
Utrecht University https://orcid.org/0000-0001-5581-5790
Ramon Oord
Utrecht University
Erik Zettler
NIOZ
Erik Van Sebille
Utrecht University https://orcid.org/0000-0003-2041-0704
Linda Amaral-Zettler
NIOZ

Physical Sciences - Article

Keywords:

Posted Date: December 2nd, 2021

DOI: https://doi.org/10.21203/rs.3.rs-955379/v1

Abstract

Millimeter- and micrometer-sized plastics are well-documented in aquatic ecosystems, but little is known about sub-micrometer particles because conventional analytical techniques lack sufficient spatial resolution or the spectroscopic means to unambiguously identify individual nanometer-sized plastic particles. We combined the spatial resolution of atomic force microscopy with chemical information from infrared spectroscopy to detect, identify, and count nanoplastics down to 20 nm in diameter in samples from different depths in the South Atlantic Ocean. We present evidence for the presence of polyethylene terephthalate (PET) nanoplastics in different states of degradation at 5000 m. Using lab-based ageing of PET, we demonstrate that nanoplastics can form even without light or interaction with the plastisphere, and that macroscopic PET items are a plausible source of PET nanoplastics in the ocean.

Main Text

Plastic pollution is a ubiquitous global problem [1,2]. Plastics have many beneficial properties, but their durability leads to persistent litter [3,4]. The effects of plastic on aquatic ecosystems are of growing concern, as more than 10 million tons enters the ocean annually [1,5]. Plastic waste is recalcitrant to microbial breakdown and fragments and degrades slowly, leading to the formation of plastic particles ranging from centimeters down to nanometers [6–11]. Most aquatic plastic litter is neither readily visible nor floating on the surface [12–14], and the generation of nanoplastics in the aquatic environment [15] and its potential impacts on the biosphere remain recognized but unquantified [9,16,17]. To date very little is known about the actual presence, origin, structure, and fate of such nanoplastics; even the size of ‘nanoplastics’ is still under debate defining it either as 1-1000 [18] or 1-100 nm [19–22]. Experimental challenges of sampling and analytical challenges of detecting plastic particles below 1 micron in size contribute to this knowledge gap.

We used photo-induced force microscopy (PiFM) for the analysis of nanoplastics, here considered plastic particles smaller than 1 micrometer. PiFM operates in non-contact atomic force microscopy (AFM) mode and records infrared (IR) spectra by sensing the dipole-dipole force attraction between sample and imaging tip when illuminated with coherent, monochromatic IR light [23,24]. In previous work this method enabled imaging and identification of plastic particles down to 20 nm in diameter [25].

In the ocean, plastic pollution is generally evaluated based on floating macro- and microplastic surface concentrations [26]. However, plastics denser than seawater (~1 g/cm^3) such as PET (1.38 g/cm^3) are thought to sink to the ocean depths [27–30]. Since the ocean water density gradually increases with depth, objects are expected to stay suspended at the depth where their density equals that of water. This fact, in combination with biofouling and remineralization [31], is offered as a plausible explanation for particle concentration at the pycnocline [32,33], where largest oceanic density gradients occur [31]. However, buoyancy or biofouling do not impact particles below a certain size, (e.g. nanometer-sized particles), but

instead their movement follows a random walk [34]. This may lead to widespread transport of nanoplastics by ocean currents [35], but experimental evidence is lacking.

Here we collected samples in the South Atlantic (-32.171° S, 6.287° E) in January 2020 (**Fig. 1a**), close to the South Atlantic Subtropical Gyre proposed to have high micro- and nanoplastic concentrations [36]. We analyzed samples from the surface (5 m), the pycnocline (60 m), and close to the ocean bottom (5170 m). Sampling, sample handling, and sample processing details with contamination prevention measures can be found in the Methods section. PiFM analysis was performed by spin coating a small volume (10 µL) of sample taken from the total sample volume of 1 L collected in glass bottles at each depth. Three technical replicates consisted of multiple scans of the wafer surface after spin coating. Assuming that the particles were equally distributed on the wafer surface after spin coating and knowing the total wafer surface area scanned during each measurement, we calculated a rough estimate of the particle concentration in the spin coated volume (see reference [25] and the Methods section for further information). No pre-processing of the seawater was performed to remove larger material. However, as PiFM provides spectroscopic information on the detected particles, it is possible to separate nanoplastics from other particles such as salt crystals [25] or non-plastic microfibers.

Figure 1b-f and Supplementary section **S2** provide unambiguous images and chemical validation for the presence of PET nanoplastic particles in the South Atlantic. We only detected PET nanoparticles close to the ocean bottom and not at any other depth. We identified one Nylon and three cellulose microfibers at the surface and one Nylon microfiber, three polystyrene (PS), and four polyethylene (PE) nanoparticles at the pycnocline. From the sum of the 5179 m-replicates, we found 12 PET nanoparticles and one PET microfiber. We also identified two PS particles at this depth. Because our sample size was low, our concentration estimates have large standard deviations and are not statistically significant (Supplementary section **S2.5**). However, given that we found nanometer-sized objects in just a fraction of 250 µL sampled from a volume as large as the ocean, our findings are noteworthy. All other samples (treated identically, including blanks) did not contain any PET nanoplastics, effectively ruling out contamination. We therefore chose PET nanoplastics which showed significant occurrence to focus on further.

Since we found PET nanoplastics exclusively close to the ocean floor, we hypothesize that sunken macro- and micro-PET might act as a local source for nanoplastic formation. At these depths PET litter is not exposed to sunlight and thus, barring biotic degradation, hydrolysis must be the major form of degradation, *i.e.* bond breakage *via* water addition [27,37–40]. To investigate this hypothesis, namely, that PET generates nanoplastics *via* hydrolysis in salt water even in the absence of light, we performed controlled laboratory degradation experiments (**Fig. 2**), by submerging pristine PET (granular microplastics of 2-4 mm) in a 35 g/L NaCl solution with a pH of ~7, *i.e.*, less basic than seawater (see also the Methods section). The sample was kept in the dark at room temperature and water was sampled after 1, 2, 4, and 8 weeks. The results of IR imaging at the 1725 cm^{-1} band, which is the characteristic C=O stretching vibration for PET, show that PiFM can unambiguously detect, identify, and quantify PET

nanoplastics at all stages of the aging experiment (**Fig. 2** and Supplementary section **S3**), confirming that PET microplastic indeed generates detectable amounts of PET nanoplastic particles even after 1 week (Supplementary **Table 4**). Significantly larger numbers of particles were detected per unit sample volume than in the seawater samples, however, as PiFM is not a high-throughput method and the number of detected PET nanoplastic particles was still low, the calculated particle concentrations remain estimates and trends in concentrations *versus* time suffer from large uncertainties. However, we managed to measure about 100 particles for each sample, which allowed us to establish particle size distributions (PSDs) (**Fig. 2bc)**. The PSDs show a shift towards smaller particle sizes with time that could indicate that fragmentation of nanoplastics continues as time progresses. Larger PET particles were flatter than smaller ones, thus deviated from a sphere in aspect ratio. This has potentially important implications for toxicology studies [25] (**Fig. 2d**) or reference materials that employ nanoscale polymer beads in laboratory studies [18,41].

We characterized a smaller subset of particles of each age group in more detail to investigate potential chemical differences, recording the full IR point spectra to establish a spectroscopic fingerprint for each particle. The multiple-particle averaged IR spectra suggest a clear correlation of the ratio of the 1740/1725 cm^{-1} bands with degradation time (**Fig. 2a** and Supplementary **Table 3**). Based on the experiment (the microplastic remained submerged), one would expect a growing standard deviation for this ratio with time as the sample after 8 weeks should contain particles of 'age' 0 to 8 weeks if particle formation proceeds linearly. This was not the case and seems in agreement with particle concentration estimates (Supplementary **Table 4**) that do not suggest a simple linear rate of formation. However, as mentioned above, the number of particles measured for each age group was not statistically sufficient to unambiguously confirm these trends.

From a chemical perspective, the IR spectra indicated partial degradation of functional groups in PET nanoplastics [42] (see also Supplementary sections **S1.1** and **S1.2**). During the aging process both the C=O stretching peak ~1725 cm^{-1} and the wagging vibration modes of the ethylene glycol segment ~1360 cm^{-1} gradually decreased in intensity, while the C=O stretching peak of terephthalic acid ~1740 cm^{-1} increased in relative intensity (**Fig. 2a** and Supplementary section **S3.1**). To confirm hydrolysis is the main degradation mechanism producing PET nanoplastics, we aged PET in a basic environment at pH=12 for 4 weeks (Supplementary section **S3.2**) to see if increased OH^- [42] concentrations enhanced degradation. Our results confirmed this: the ratio of the 1740/1725 cm^{-1} bands increased significantly compared to the experiment at pH=7 (**Fig. 2a**). The particle concentration estimates were not fully conclusive: one sample at pH 12 (although the statistically more significant one) showed much higher particle numbers, while the other sample, where only a very small wafer surface area was measured, did not (**Fig. 2c**). We propose that the aging experiments performed at pH=7 may even underestimate the degradation rate in seawater (pH ~8, room temperature). Interestingly, the PSD after 4 weeks was very similar for both experiments, suggesting a more complex interplay between rate of formation and particle morphology.

With our experimental evidence for the formation of nanoplastics from microplastics in salt water in the dark, we compared the full PiFM IR point spectra of individual PET nanoplastic particles from the South Atlantic water samples (**Fig. 3**) with those obtained for lab-generated PET nanoplastics. The spectral differences we observed between ocean samples were very similar to the ones recorded for the lab-generated PET nanoplastics with different aging times (**Fig. 2a** and Supplementary section **S3.1**). Based on the correlation, we established above between the increase of the band ratio 1740/1725 cm^{-1} with ageing time, we therefore suggest that the PET nanoplastics we identified in the ocean are in different stages of degradation. Assuming more or less constant conditions for hydrolysis of PET at the ocean bottom, we speculate that particle 2 in **Fig. 3ab** is 'younger' than particle 3 in **Fig. 3cd** based on their respective spectra (**Fig. 3g**).

However we interpret this observation with caution since PET degradation is a complex process [42] and in order to establish a more quantitative age classification of individual PET nanoplastic particles, we would need to assess a larger spectral range, and considering other factors such as molecular orientation effects (see, for example, Supplementary section **S3.4** reporting experiments we performed with polarized light). Furthermore, as we found PET nanoparticles only in water samples collected close to the ocean bottom, future lab-based ageing experiments need to consider the lower temperature (< 4°C) and higher pressure experienced at these depths [43]. Nevertheless, the results we report here show that such age classification may be possible, introducing new ways for tracing the origin and fate of marine nanoplastics. As nanoplastics below a certain size behave distinctly, knowledge of their age alongside that of ocean currents transporting them enables both their point of origin, as well as potential sinks for PET nanoplastic particles, completing existing models for transport of macro- and microplastics [35].

Conclusion

In conclusion, we show unambiguous evidence for the presence of PET nanoplastics in the South Atlantic Ocean at 5179 m depth. We did not detect any PET nanoplastics at the ocean surface or in the pycnocline (60 m) but did find PS nanoplastics both in the pycnocline and close to the ocean bottom and PE nanoplastics only in the pycnocline layer. At the ocean surface, we only detected cellulose (*e.g.* cotton) and Nylon microfibers; the latter was also found in the pycnocline. The method we used to count nanoplastics can unambiguously identify and speciate nanoplastic particles down to ~20 nm in size but it is a low-throughput method and particle concentration estimates show large standard deviations. The comparison of the spectroscopic fingerprints of individual PET nanoplastic particles found close to the ocean floor with data obtained *via* controlled ageing of PET provided a PET age distribution and confirmed hydrolysis as a formation mechanism. Interestingly, we also found two PS particles at this depth. PS macro- and microplastics may sink to the ocean floor if their density is high enough, for example in the case of crystal-grade PS (~1.05 g/cm^3) [32]. Alternatively, lower density PS (< 1 g/cm^3) or foam expanded PS (~0.05 g/cm^3) will not sink [32] and in that case, transport of nanoplastics *via* ocean currents could play a role in the 3D distribution of nanoplastics in the oceans as well. Finally, it is important to note that most nanoplastics we detected (see Supplementary section **S2**) were aggregated

with non-plastic material. This complicates collection *via* filtration since, as most of these particles, although significantly smaller than 500 nm, would be missed with pre-filters with pore sizes of 500 nm or greater. Likewise, the true concentrations of nanoplastics would be largely underestimated.

References

1. Kane, I. A. *et al.* Seafloor microplastic hotspots controlle by deep-sea circulation. *Science* **368**, 1140–1145 (2020).

2. Mitrano, D. M., Wick, P. & Nowack, B. Placing nanoplastics in the context of global plastic pollution. *Nat. Nanotechnol.* **16**, 491–500 (2021).

3. UNEP 2009. *Marine Litter: A Global Challenge*. (2009).

4. Bergmann, M., Gutow, L. & Klages, M. *Marine anthropogenic litter*. *Marine Anthropogenic Litter* (Springer Nature, 2015).

5. Jambeck, J. R. *et al.* Plastic waste inputs from land into the ocean. *Science* **347**, 768–771 (2015).

6. Klemchuk, P. P. Degradable plastics: A critical review. *Polym. Degrad. Stab.* **27**, 183–202 (1990).

7. Thompson, R. C. *et al.* Lost at Sea: Where Is All the Plastic? *Science* **304**, 838 (2004).

8. Barnes, D. K. A., Galgani, F., Thompson, R. C. & Barlaz, M. Accumulation and fragmentation of plastic debris in global environments. *Philos. Trans. R. Soc. B Biol. Sci.* **364**, 1985–1998 (2009).

9. Cole, M., Lindeque, P., Halsband, C. & Galloway, T. S. Microplastics as contaminants in the marine environment: A review. *Mar. Pollut. Bull.* **62**, 2588–2597 (2011).

10. Cózar, A. *et al.* Plastic debris in the open ocean. *Proc. Natl. Acad. Sci. U. S. A.* **111**, 10239–10244 (2014).

11. Eriksen, M. *et al.* Plastic Pollution in the World's Oceans: More than 5 Trillion Plastic Pieces Weighing over 250,000 Tons Afloat at Sea. *PLoS One* **9**, 1–15 (2014).

12. Van Sebille, E. *et al.* A global inventory of small floating plastic debris. *Environ. Res. Lett.* **10**, 1–11 (2015).

13. Hardesty, B. D. *et al.* Using numerical model simulations to improve the understanding of micro-plastic distribution and pathways in the marine environment. *Front. Mar. Sci.* **4**, 1–9 (2017).

14. Ter Halle, A. *et al.* Understanding the Fragmentation Pattern of Marine Plastic Debris. *Environ. Sci. Technol.* **50**, 5668–5675 (2016).

15. Gigault, J., Pedrono, B., Maxit, B. & Ter Halle, A. Marine plastic litter: The unanalyzed nano-fraction. *Environ. Sci. Nano* **3**, 346–350 (2016).

16. Andrady, A. L. Microplastics in the marine environment. *Mar. Pollut. Bull.* **62**, 1596–1605 (2011).

17. Gigault, J. *et al.* Nanoplastics are neither microplastics nor engineered nanoparticles. *Nat. Nanotechnol.* **16**, 501–507 (2021).

18. Gigault, J. *et al.* Current opinion: What is a nanoplastic? *Environ. Pollut.* **235**, 1030–1034 (2018).

19. Jahnke, A. *et al.* Reducing Uncertainty and Confronting Ignorance about the Possible Impacts of Weathering Plastic in the Marine Environment. *Environ. Sci. Technol. Lett.* **4**, 85–90 (2017).

20. Ferreira, I., Venâncio, C., Lopes, I. & Oliveira, M. Nanoplastics and marine organisms: What has been studied? *Environ. Toxicol. Pharmacol.* **67**, 1–7 (2019).

21. Alimi, O. S., Farner Budarz, J., Hernandez, L. M. & Tufenkji, N. Microplastics and Nanoplastics in Aquatic Environments: Aggregation, Deposition, and Enhanced Contaminant Transport. *Environ. Sci. Technol.* **52**, 1704–1724 (2018).

22. Schwaferts, C., Niessner, R., Elsner, M. & Ivleva, N. P. Methods for the analysis of submicrometer- and nanoplastic particles in the environment. *Trends Anal. Chem.* **112**, 52–65 (2019).

23. Nowak, D. *et al.* Nanoscale chemical imaging by photoinduced force microscopy. *Sci. Adv.* **2**, e1501571 (2016).

24. Dazzi, A. & Prater, C. B. AFM-IR: Technology and applications in nanoscale infrared spectroscopy and chemical imaging. *Chem. Rev.* **117**, 5146–5173 (2017).

25. C. ten Have, I. *et al.* Photoinduced Force Microscopy as an Efficient Method Towards the Detection of Nanoplastics. *Chemistry–Methods* **1**, 205–209 (2021).

26. Ter Halle, A. *et al.* Nanoplastic in the North Atlantic Subtropical Gyre. *Environ. Sci. Technol.* **51**, 13689–13697 (2017).

27. Gerritse, J., Leslie, H. A., de Tender, C. A., Devriese, L. I. & Vethaak, A. D. Fragmentation of plastic objects in a laboratory seawater microcosm. *Sci. Rep.* **10**, 1–16 (2020).

28. Zhang, C. *et al.* Microplastics in offshore sediment in the Yellow Sea and East China Sea, China. *Environ. Pollut.* **244**, 827–833 (2019).

29. Zhang, F. *et al.* Composition, spatial distribution and sources of plastic litter on the East China Sea floor. *Sci. Total Environ.* **742**, 140525 (2020).

30. Kanhai, L. D. K. *et al.* Microplastics in sub-surface waters of the Arctic Central Basin. *Mar. Pollut. Bull.* **130**, 8–18 (2018).

31. Kooi, M., Van Nes, E. H., Scheffer, M. & Koelmans, A. A. Ups and Downs in the Ocean: Effects of Biofouling on Vertical Transport of Microplastics. *Environ. Sci. Technol.* **51**, 7963–7971 (2017).

32. Pabortsava, K. & Lampitt, R. S. High concentrations of plastic hidden beneath the surface of the Atlantic Ocean. *Nat. Commun.* **11**, 1–11 (2020).

33. Choy, C. A. *et al.* The vertical distribution and biological transport of marine microplastics across the epipelagic and mesopelagic water column. *Sci. Rep.* **9**, 1–9 (2019).

34. De La Fuente, R., Drótos, G., Hernández-García, E., López, C. & Van Sebille, E. Sinking microplastics in the water column: Simulations in the Mediterranean Sea. *Ocean Sci.* **17**, 431–453 (2021).

35. Wichmann, D., Delandmeter, P. & van Sebille, E. Influence of Near-Surface Currents on the Global Dispersal of Marine Microplastic. *J. Geophys. Res. Ocean.* **124**, 6086–6096 (2019).

36. Ryan, P. G. Does size and buoyancy affect the long-distance transport of floating debris? *Environ. Res. Lett.* **10**, (2015).

37. Mattsson, K., Hansson, L. A. & Cedervall, T. Nano-plastics in the aquatic environment. *Environ. Sci. Process. Impacts* **17**, 1712–1721 (2015).

38. Zettler, E. R., Mincer, T. J. & Amaral-Zettler, L. A. Life in the “Plastisphere”: Microbial Communities on Plastic Marine Debris. *Environ. Sci. Technol.* **47**, 7137–7146 (2013).

39. Stanica-Ezeanu, D. & Matei, D. Natural depolymerization of waste poly(ethylene terephthalate) by neutral hydrolysis in marine water. *Sci. Rep.* **11**, 1–7 (2021).

40. Keinänen, O. *et al.* Harnessing PET to track micro- and nanoplastics in vivo. *Sci. Rep.* **11**, 1–12 (2021).

41. Wagner, S. & Reemtsma, T. Things we know and don’t know about nanoplastic in the environment. *Nat. Nanotechnol.* **14**, 300–301 (2019).

42. Sammon, C., Yarwood, J. & Everall, N. FT-IR study of the effect of hydrolytic degradation on the structure of thin PET films. *Polym. Degrad. Stab.* (2000).

43. Safarov, J. *et al.* (p,ρ,T) properties of seawater Extensions to high salinities. *Deep. Res. Part I* **65**, 146–156 (2012).

Declarations

Funding F.M., L.A.A-Z., E.v.S., and B.M.W. acknowledge financial support from the Netherlands Organisation for Scientific Research (NWO) in the frame of an NWO Groot project (OCENW.GROOT.2019.043). B.M.W. acknowledges financial support from the Netherlands Organisation for Scientific Research (NWO) in the frame of the Advanced Research Center (ARC) Chemical Building Blocks Consortium (CBBC). E.v.S. acknowledges financial support from the European Research Council (ERC) under the European Union's Horizon 2020 research and innovation programme (grant agreement No 715386).

Author contributions F.M. and B.M.W. initiated the idea of detecting nanoplastics with PiFM and guided the research. F.M. initiated the idea of lab-based PET degradation. I.C.t.H. prepared all the samples and performed the PiFM and IR analyses. R.O. went on the RV *Pelagia* cruise and collected all the ocean samples. L.A.A.Z arranged and led the RV *Pelagia* cruise, and along with E.R.Z, and E.v.S. participated in scientific discussions. F.M. and I.C.t.H. made the figures and wrote the first version of the manuscript, which was then revised by all authors for the final article.

Competing interests The authors declare no competing interests.

Additional information

Supplementary information is available for this paper at …

Reprints and permissions information is available at …

Correspondence and requests for materials should be addressed to F.M. or B.M.W.

Methods

Sample collection, handling, and preparation. Samples were collected during research cruise 64PE448 onboard the *RV PELAGIA*, from the South Atlantic at -32.171° S and 6.287° E. At this location water was collected from different depths using a Rosette sampler equipped with a CTD (Conductivity, Temperature and Depth) sensing system (Seabird SBE21) [1]. Before deploying the Rosette system, the bottles were thoroughly cleaned to avoid contamination: 1L glass sample bottles were thoroughly rinsed using ultra-pure (UPW) water before they were filled straight from the Rosette system, to reduce contamination. The UPW used for cleaning was also checked for impurities using the same measurement procedure as for ocean water samples, but no contamination was found. Besides, the UPW was used to make blanks that were treated in the exact same way as the samples from the ocean. No nanoplastics were found in the blanks.

We sampled from the surface (5 m depth), the pycnocline at 60 m depth and the bottom layer at 5179 m depth. For Photo-induced force microscopy (PiFM) analysis 10 µL of sample was drop casted without any pretreatment using a Finnpipette (Thermo Fischer Scientific; polypropylene tips) and spin coated onto

~7x7 mm SiO_2/Si(100) wafers (sample carriers) that had been cleaned as described previously. Spin coating was performed at 3000 rpm for 30 s using an Ossila spin coater operated in a fume hood.

Avoiding contamination. During transit, the samples were kept in closed glass bottles. All sample preparation steps were performed in the air-controlled environment of a laminar flowhood. Cotton clothing was worn at all times, as cotton fibers can easily be distinguished from nanoplastics with PiFM. All labware used, such as beakers, vials, and syringes, was made of glass. The Finnpipette tips were made of polypropylene (PP) (Thermo Fischer Scientific). Even though we did not detect any PP, this polymer could easily be distinguished from polyethylene terephthalate (PET) in the photo-induced force microscopy (PiFM) measurements. Auxiliary equipment, such as tweezers and spatulas were made of stainless steel. Equipment was always rinsed 3 times with UPW, before usage. UPW was also measured as a reference, and we did not find any nanoplastics. To make sure the SiO_2/Si(100) wafers (sample carriers) were pristine before usage, they were ultrasonicated in a H_2O/EtOH/acetone mixture (1:1:1 v/v), washed and ultrasonicated in deionized water, heated to 40°C in $H_2O/NH_4OH/H_2O_2$ (5:1:1 v/v), washed with deionized H_2O and then boiled in deionized H_2O. The pristine wafers were stored in deionized water or ethanol. Before usage they were baked at 120°C and cleaned with UV/Ozone.

Photo-induced Force Microscopy. Photo-induced force microscopy (PiFM) was performed and analyzed using a VistaScope photo-induced force microscope (PiFM) from Molecular Vista (San Jose, CA, USA). This instrument is equipped with a quantum cascade laser (QCL) unit and IR spectra were recorded in the 775-1950 cm^{-1} range. Atomic force microscopy (AFM) topography images were recorded in non-contact mode together with PiFM maps and IR point spectra (60 accumulations of 500 ms with 1 cm^{-1} spectral resolution). Additionally, hyperspectral maps, with every pixel being a full IR spectrum, were recorded. Typical image sizes were 1-400 μm^2 with a spatial resolution of 10-15 nm, dependent on the size of the AFM tip, and a probing depth of ~30 nm. The data were analyzed with the VistaScan 1.7, SurfaceWorks 2.4 software, Origin 9, and MATLAB.

PiFM machine calibration using varying sizes of polystyrene (PS) Nanospheres (Thermo Fischer Scientific) can be found in reference [2].

Particle size distributions (PSD) and particle concentration estimates of nanoplastics from PiFM measurements have been performed as detailed in reference [2] and summarized in Supplementary section S3.3.

PiFM IR reference spectra were recorded for PET, PS, and polyethylene (PE). For this, granular macroplastic pieces (PET) and beads (PS, PE) in the size range of 2-4 mm (Sigma-Aldrich) were used. The plastic pieces were cut using a stainless-steel knife (Stanley) in order to create a smooth surface suitable for PiFM measurements. For all polymers, 3 hyperspectral images were recorded (1-4 μm^2) and the average of these 3 images was used as reference PiFM IR spectrum.

Lab-generated polyethylene terephthalate (PET) nanoplastics. The nanoplastics were prepared by aging PET (granular macroplastic pieces in the size range of 2-4 mm) in NaCl solutions. 280 mg NaCl was dissolved in 8 mL deionized water and 160 mg of PET (Sigma-Aldrich) was added to the solution (pH=7). For samples studied at pH=12, NaOH pellets (Alfa Aesar) were added to increase the pH to a value of 12. The pH was measured with a TitraLab AT1000 Series (HACH) pH meter. After aging for 1, 2, 4, and 8 weeks, always 10 µL of solution were drop casted with a Finnpipette (Thermo Fischer Scientific; polypropylene (PP) tips) and spin coated onto ~7x7 mm SiO_2/Si(100) wafers at 3000 rpm for 30 s (Ossila spin coater operated in a fume hood).

Attenuated Total Reflection – Infrared spectroscopy. Attenuated total reflection-infrared spectroscopy (ATR-IR) reference spectra of bulk PET, PS, and PE (Sigma-Aldrich) were recorded using a PerkinElmer FT-IR spectrometer 'Frontier'. The spectra were recorded at room temperature in the 400-4000 cm^{-1} range (32 accumulations of 500 ms with 2 cm^{-1} spectral resolution).

The band assignments of reference IR spectra are displayed in Supplementary **Fig. 1** and listed in Supplementary **Table 1**.

Data availability

The data that support the findings of this study are available within the paper and its Supplementary Information, and all data are available from the authors on reasonable request.

Methods References

1. Kanhai, L. D. K. *et al.* Microplastics in sub-surface waters of the Arctic Central Basin. *Mar. Pollut. Bull.* **130**, 8–18 (2018).

2. ten Have, I. C. *et al.* Photoinduced Force Microscopy as an Efficient Method Towards the Detection of Nanoplastics. *Chemistry–Methods* **1**, 205–209 (2021).

Figures

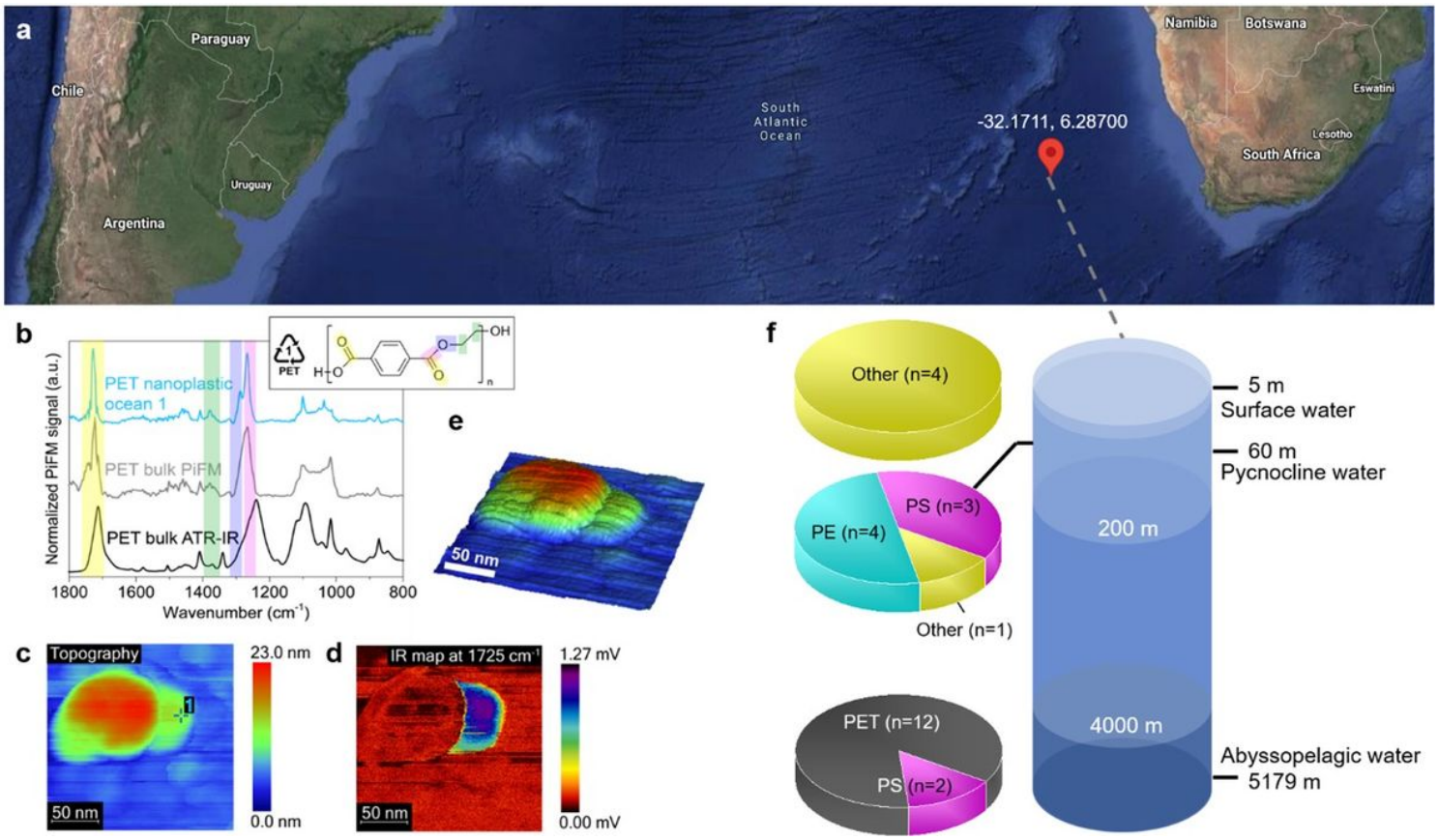

Figure 1

Studying individual nanoplastics in the South Atlantic Ocean with photo-induced force microscopy (PiFM). a, Sampling location in the South Atlantic Ocean close to Cape Basin. b, Infrared spectra of a polyethylene terephthalate (PET) bulk reference, obtained with attenuated total reflectance – infrared (ATR-IR) spectroscopy and PiFM, and of a PET nanoplastic particle (1) found at 5179 m depth. c, Topography map of -PET nanoplastic 1 and d, corresponding IR map recorded at the characteristic C=O stretching vibration of PET at 1725 cm-1. The location of the PiFM IR point spectrum from b, is indicated in the topography map by the label ‘1’. e, 3D topography map of the particles from c, indicating how the nanoplastic particle is half covered by another non-plastic particle. f, Depth profile of the sampling location and the types of nanoplastics detected at every depth.

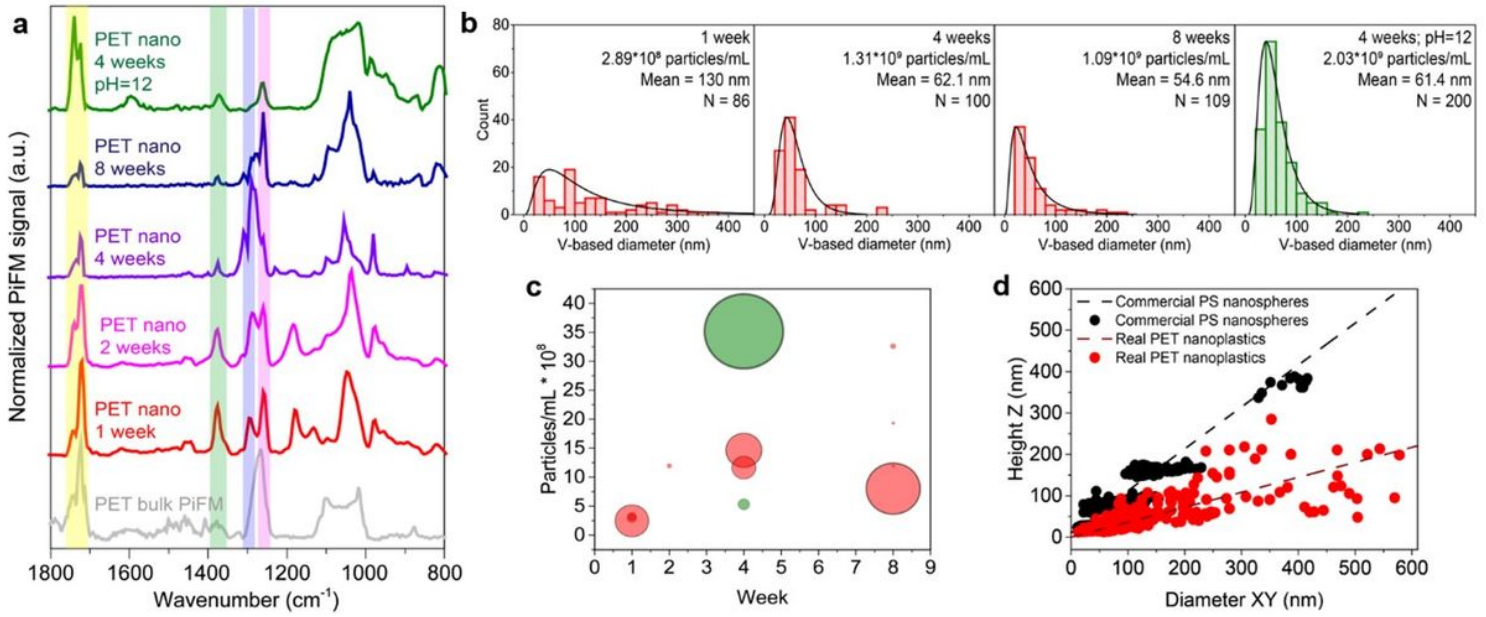

Figure 2

Studying individual polyethylene terephthalate (PET) nanoplastics in the laboratory. a, PiFM IR spectra of PET nanoplastics created after 1, 2, 4, and 8 weeks of microplastic degradation in salt water at pH=7, as well as after 4 weeks in salt water at pH=12. The PiFM IR spectrum of bulk PET (gray line) was added as a reference. The colored regions in the spectra indicate the C=O stretching peak (yellow), the wagging vibration modes of the ethylene glycol segment (green), the C-O stretching vibrations (blue), and the vibrations from the terephthalate group (magenta). b, Particle size distributions (PSDs) of PET nanoplastics after 1, 4, and 8 weeks of microplastic degradation in salt water at pH=7, as well as after 4 weeks in salt water at pH=12. c, PET nanoplastic concentrations over time during the degradation experiments as estimated per measurement. The size of the bubbles scales with the number of particles found per measurement. The pH=7 sample is indicated in red and the pH=12 sample in green. d, Height in Z dimension of all PET nanoplastic particles (red) and polystyrene (PS) size standards 25 (black) plotted versus the particles' XY diameter.

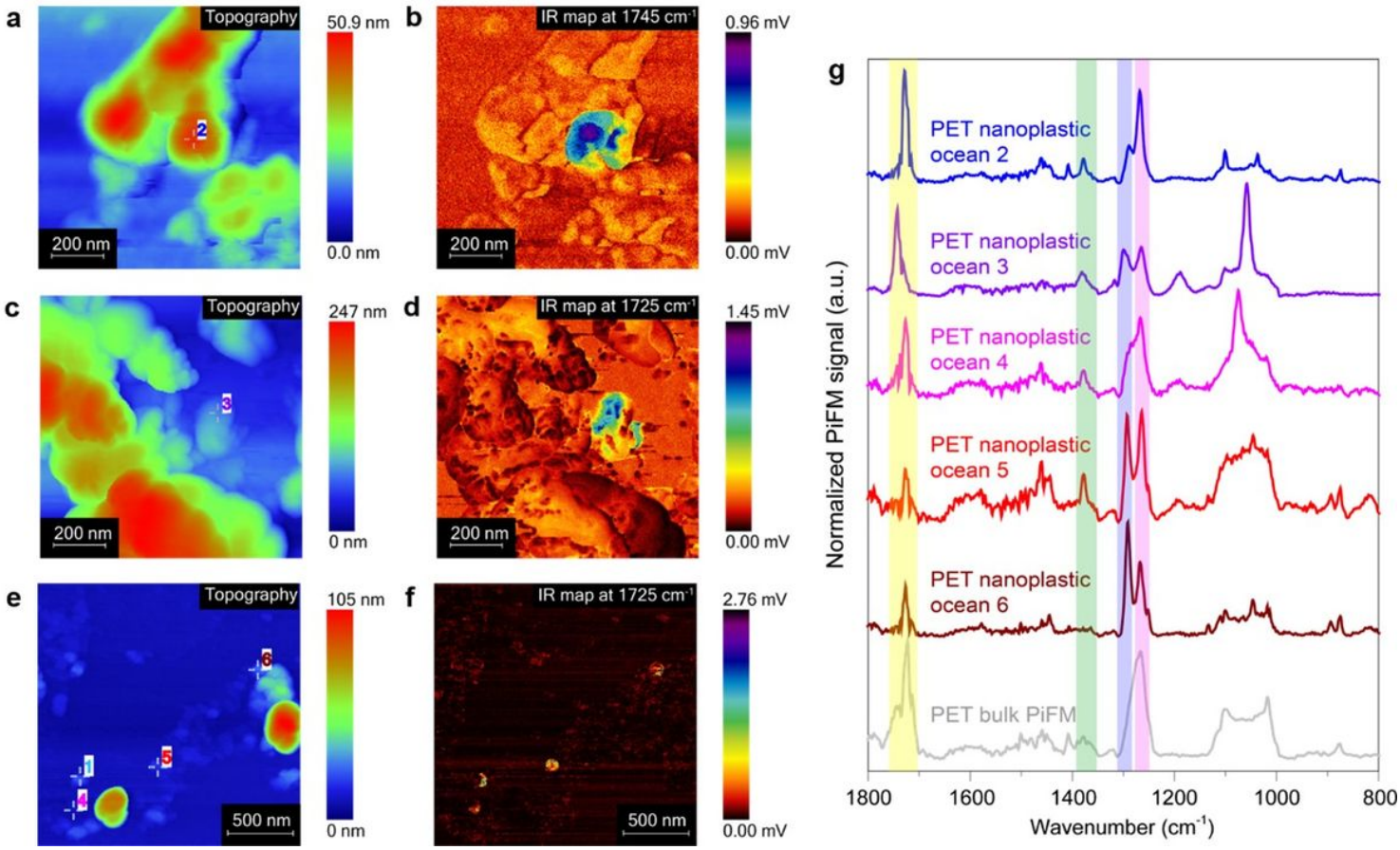

Figure 3

PET nanoplastics near the bottom of the South Atlantic Ocean. a, c, e, Topographic images and b, d, f, IR maps recorded at the characteristic C=O stretching vibrations at 1725 and 1745 cm-1 of PET nanoplastics found at 5179 m depth. g, PiFM IR point spectra of the PET nanoplastics (2-6) depicted in a-f. The locations of the PiFM IR point spectra are indicated in the topography maps with 2-6. The PiFM IR spectrum of PET nanoplastic 1 can be found in Figure 1b. The PiFM IR spectrum of bulk PET (gray line) was added as a reference. The colored regions in the spectra indicate the C=O stretching peak (yellow), the wagging vibration modes of the ethylene glycol segment (green), the C-O stretching vibrations (blue), and the vibrations from the terephthalate group (magenta).

Supplementary Files

This is a list of supplementary files associated with this preprint. Click to download.

- SINanoplasticsPETandoceanfinal.docx